

A CRF-based Framework for Tracklet Inactivation in Online Multi-Object Tracking

Tianze Gao, Huihui Pan, Zidong Wang, *Fellow, IEEE*, and Huijun Gao, *Fellow, IEEE*

Abstract—Online multi-object tracking (MOT) is an active research topic in the domain of computer vision. In this paper, a CRF-based framework is put forward to tackle the tracklet inactivation issues in online MOT problems. We apply the proposed framework to one of the state-of-the-art online MOT trackers, Tracktor++. The baseline algorithm for online MOT has the drawback of simple strategy on tracklet inactivation, which relies merely on tracking hypotheses' classification scores partitioned by using a fixed threshold. To overcome such a drawback, a discrete conditional random field (CRF) is developed to exploit the intra-frame relationship between tracking hypotheses. Separate sets of feature functions are designed for the unary and binary terms in the CRF so as to cope with various challenges in practical situations. The hypothesis filtering and dummy nodes techniques are employed to handle the problem of varying CRF nodes in the MOT context. In this paper, the inference of CRF is achieved by using the loopy belief propagation algorithm, and the parameters of the CRF are determined by utilizing the maximum likelihood estimation method. Experimental results demonstrate that the developed tracker with our CRF-based framework outperforms the baseline on the MOT16 and MOT17 datasets. The extensibility of the proposed method is further validated by an extensive experiment.

Index Terms—Conditional random field, Online multi-object tracking, Tracklet inactivation

I. INTRODUCTION

MULTI-OBJECT tracking (MOT) has become a popular research topic attracting an ever-increasing interest from the computer vision community due to its wide application potential. In general, MOT algorithms can be categorized into the online algorithms and the offline ones based on whether the incorporation of the information from future frames is carried out or not. Compared with their offline counterparts, online algorithms are more suited for real time applications including autonomous driving and mobile robotics. Currently, the mainstream MOT paradigm is tracking-by-detection, which presents a two-step solution to the MOT problem: 1) discover objects of interest through a detector; and 2) form trajectories by using the data association method. It should be mentioned that the tracking-by-detection paradigm is heavily dependent on the detection quality, and an additional feature extractor is usually required to compute the appearance affinity. Another trend in MOT follows the

paradigm of tracking-by-SOT, wherein SOT stands for the single object trackers. The correlation filter based tracking methods fall into the tracking-by-SOT paradigm.

As one of the most promising online trackers in MOT, the Tracktor++ proposed in [1] follows the tracking-by-detection paradigm. In the Tracktor++, a faster region-based convolutional network (Faster R-CNN) is employed as the object detector [2]. The existing tracklets are extended by using the regression head of the detector. Although the Tracktor++ has achieved top performance in view of CLEAR MOT metrics [3], there are still some drawbacks in this algorithm. As is shown in Fig. 1, one drawback of the Tracktor++ comes from the unreliable judgment of the moment for inactivating a tracklet. Tracklets are inactivated when the tracking hypotheses are missing or unreliable. For online MOT problems, inactivating a tracklet means that a tracklet is temporarily removed from the current tracklet list while keeping its potential qualification to be reidentified. Most current online MOT algorithms would predefine a life span for each tracklet to determine the maximal number of continuous inactivation frames before it is thoroughly deleted.

In the Tracktor++, a tracklet is inactivated when the corresponding classification score is below a certain threshold, which can be problematic in some cases (especially when a tracking target is leaving the image boundary). We argue that such tracking errors can be alleviated by considering not only the information of individual tracking hypotheses, but also the intra-frame relationship between the tracking hypotheses. In this paper, a discrete conditional random field (CRF) is employed to solve the improper tracklet inactivation problem. Since the tracklet inactivation mechanism is totally decoupled from the main tracking pipeline of Tracktor++, our method can be transferred to trackers with a similar architecture, namely trackers remoulded from detectors, which indicates that our method has wider application potential than Tracktor++.

Two concerns come up when using a CRF in the MOT context: i) the number of CRF nodes is varying according to the detected objects in a certain frame, whereas the traditional formulation of the CRF is built upon a fixed set of nodes; and ii) the overfitting problem may occur during the training process under the condition that the scale of the training dataset is relatively small with respect to the number of CRF parameters. In this context, two strategies are adopted to address the aforementioned concerns. On the one hand, the hypothesis filtering and dummy nodes are applied to fix the number of CRF nodes. On the other hand, the graph factors are divided into the unary and binary groups. Then, the parameter sharing strategy is utilized within each of the two groups,

T. Gao, H. Pan, H. Gao are with the Research Institute of Intelligent Control and Systems, Harbin Institute of Technology, Harbin, 150001, China.

Z. Wang is with the Department of Computer Science, Brunel University London, Uxbridge, Middlesex, UB8 3PH, United Kingdom.

Huijun Gao is the corresponding author (e-mail: hjgao@hit.edu.cn).

This work has been submitted to the IEEE for possible publication. Copyright may be transferred without notice, after which this version may no longer be accessible.



Fig. 1: Examples for the improper tracklet inactivation in Tracktor++. The tracking hypotheses in red boxes drift to nearby objects as a consequence. This is a common problem happening in Tracktor++ and most other trackers that follow the tracking-by-SOT paradigm.

which effectively reduces the risk of overfitting.

In the proposed method, the tracking objects in the scene are treated equally (i.e. no object is considered to be more special than others), and thus, the CRF is constructed in a fully connected way. The loopy belief propagation algorithm proposed in [4] is applied for the inference phase. For the training phase, the maximum likelihood estimation method is adopted and the stochastic gradient descent (SGD) algorithm is utilized to update the parameters.

The main contributions of this paper can be summarized as follows:

- A discrete CRF-based framework is developed to handle the unreliable judgment for the tracklet inactivation problem of the Tracktor++.
- The feature functions for unary and binary terms are designed to cope with multiple concerns encountered in practical situations.
- An effective mechanism is put forward for tracklet inactivation, which outperforms the traditional threshold method.
- Experiments are conducted on two benchmarks MOT16 and MOT17. Experimental results demonstrate the superiority of the developed CRF-based method over the baseline method.
- The extensibility of the proposed framework is validated by conducting an extensive experiment.

The rest of this paper is organized as follows. The background of the MOT problem is introduced in Section II. In Section III, the details of the proposed framework are presented. The experimental settings are discussed in Section IV. The

details of performance indicators, experimental results and an extensive experiment are provided in Section V. Conclusions are drawn in Section VI.

II. RELATED WORK

During the past few decades, MOT has become a research focus in computer vision. In this section, we briefly review the MOT methods that leverage the power of machine learning and those with the aid of CRF.

A. MOT with Machine Learning

Machine learning approaches have proven to be effective for dealing with the MOT problems through years of practice. The most popular paradigm in this direction is tracking-by-detection [5], [6]. The interested objects are firstly detected by using a deep convolutional neural network. The affinity scores based on appearance and motion information of the objects are then computed. Finally, the objects are correlated through data association. One of the first algorithms that follows this paradigm is the Simple Online and Realtime Tracking (SORT) algorithm [7] which uses the Kuhn–Munkres algorithm [8] for data association and a Kalman filter [9] for observation correction. DeepSORT has been proposed in [10] to further improve SORT by learning a deep association metric in visual appearance space. Zhou et al. [11] have enhanced the tracking accuracy by using a deep alignment network. In addition, a local-to-global strategy for robust data association has been introduced in [12]. In recent years, some dedicated tracking algorithms have been designed either to increase the recall and

accuracy of the detector, or to enhance the performance of data association [13]–[18].

Another line of work follows the paradigm of tracking-by-SOT, which assigns an individual single object tracker for each tracking target. The approaches following this paradigm are effective because single object trackers often pay more attention to the similarity between nearby image patches in consecutive frames than to the integrity of semantic information. Hence, some objects that the detector fails to discover can be recognized by using the single object trackers. This point of view holds particularly well in the trackers based on correlation filters. For example, the kernelized correlation filters (KCF) proposed in [19] has been employed to solve the MOT problems [20]. In [21], the efficient convolution operators (ECOs) proposed in [22] have been utilized for dealing with the MOT problems with remarkable performance.

The state-of-the-art tracker, Tracktor++ [1], generally falls into the paradigm of tracking-by-detection. It leverages a Faster R-CNN to discover new tracking targets. Notice that the positions of confirmed tracking objects are regressed in later frames by using the regression head of the Faster R-CNN, which differs from the traditional tracking-by-detection approaches. Using such a tracking pipeline, a challenge is the necessity to reasonably inactivate a tracklet in case it drifts to uninterested regions. In Fig. 1, we can see that the simple strategy adopted in [1] is unreliable, which needs to be improved.

B. MOT with CRF

CRF models are frequently used in Natural Language Processing (NLP) and visual segmentation tasks. The advantage of CRF is its strong ability to model the complex interactions between individuals. Therefore, CRF has been utilized to solve MOT problems.

Most research works on CRF-based methods are geared towards offline MOT problems, i.e. information from future frames is available to be utilized. Yang et al. [23] have built a fully connected CRF model that associated short tracklets to form long ones. The CRF edges have been designed to focus on discriminating spatially close targets with similar appearances. Heili et al. [24] have exploited long-term connectivity between different detections. Multiple cues have been extracted to measure the similarity and dissimilarity when formulating the energy potentials. A recent work [25] has followed the basic ideas of [23], whereas it learns the pairwise potentials by using a bidirectional long short-term memory (LSTM) network, and approximated the inference phase of the CRF by using a recurrent neural network (RNN). The entire tracking pipeline is thus differentiable and can be trained end-to-end.

By contrast, the application of CRF in online MOT problems has not yet been fully studied. Zhou et al. [26] have proposed a method to solve the MOT problem in an online way. In [26], the displacements between consecutive frames have been first estimated by using a dedicated neural network. Then, a deep continuous CRF with asymmetric pairwise terms has been utilized to refine the displacements. Note that our

method is different from [26] in that we use a discrete CRF to judge the inactivation of tracklets instead of directly interacting with the positions of tracking hypotheses. Besides, since our framework is decoupled from the main tracking pipeline, it is featured with flexibility and extensibility in the sense of being applied to more advanced algorithms in the future.

III. METHOD

In this section, we first make a brief description for the baseline tracker, Tracktor++. After that, the formulation of the proposed CRF framework is presented. Then, we show how the feature functions are designed by taking the interaction between different targets into account. Finally, the method for CRF inference and parameter estimation is introduced, including the two techniques employed to keep the number of CRF nodes fixed.

A. Baseline Tracker

The tracking pipeline of the baseline tracker, also known as Tracktor++, is depicted in Fig. 2. As a tracking-by-detection method, the tracking objects of interest are detected by a Faster R-CNN detector. With the arrival of each new frame, the latest bounding box of each tracklet is treated as the region proposal and sent to the regression and classification heads. The new positions and scales of the tracklets are then provided by the output of the regression head. Once the classification score of a tracklet is lower than a predefined threshold, the tracklet is inactivated. The new detections that are covered by tracklets are filtered out by non-maximum suppression. An individual siamese network is also employed to reidentify the previously inactivated tracklets. Finally, the remaining detections are treated as the starting points of new tracklets.

B. Problem Formulation

The general architecture of our developed method is illustrated in Fig. 2, where the state-of-the-art method, Tracktor++, is used as the baseline. Given a set of K regressing results $x^t = \{x_1^t, x_2^t, \dots, x_K^t\}$, our goal is to make a reasonable judgment $y^t = \{y_1^t, y_2^t, \dots, y_K^t\}$ labeling whether the tracklets should be inactivated. Here, we use $x_i^t = \{S_i^t, m_i^t, l_i^t\}$ as the ensemble tracking information of the tracklet i at frame t , including the classification score S_i^t , the motion information m_i^t and the size information l_i^t . We will omit the frame index t for simplicity in the following formalism.

We model the inactivation labeling problem with a CRF which is factorized as a factor graph [27] $G = (V, F, \mathcal{E})$, where $V = \{1, 2, \dots, K\}$ is the set of nodes corresponding to the tracklet indices. F and \mathcal{E} are the sets of factors and edges in the graph respectively. The joint conditional distribution can thus be expressed as

$$p(y|x; \theta) = \frac{1}{Z(x; \theta)} \prod_{f \in F} e^{-E_f(x, y; \theta)}, \quad (1)$$

with

$$Z(x; \theta) = \sum_{y \in Y} \prod_{f \in F} e^{-E_f(x, y; \theta)}, \quad (2)$$

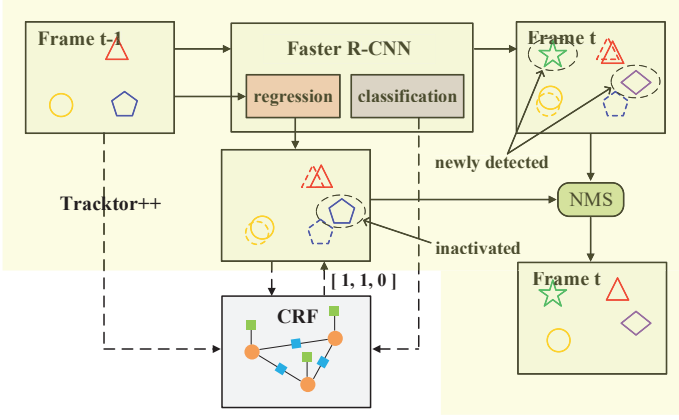


Fig. 2: The architecture of our method. We pose the judgement for tracklet inactivation as a binary labeling problem, where label 0 indicates the tracklet should be inactivated and label 1 indicates the contrary. The labeling output is jointly determined by the unary and binary terms of the CRF model. In this example, the tracking hypothesis represented by the pentagon is inactivated and removed from the final tracking result.

where Y denotes the domain of y . E_f is the energy function of the factor f .

Note that the dataset exploited for training the CRF is established by using the improper inactivation instances produced by Tracktor++ as negative samples. Such instances simply produce a small scale dataset. Thereby, parameter sharing is applied to our method to prevent the overfitting problem. This is achieved by grouping the factors in (1) by a set of two cliques $C = \{C_u, C_b\}$, i.e., a unary one and a binary one. Then, we have

$$p(y|x; \theta) = \frac{1}{Z(x; \theta)} \prod_{C_F \in C} \prod_{f \in C_F} e^{-E_f(x_f, y_f; \theta_f)}. \quad (3)$$

Defining $E_f(x, y_f; \theta_f) = \theta_f \Phi_f(x, y_f)$, we have a more detailed form of (3) as follows

$$p(y|x; \theta) = \frac{1}{Z(x; \theta)} e^{\theta_u \sum_{f \in C_u} \Phi_u(x_f, y_f) + \theta_b \sum_{f \in C_b} \Phi_b(x_f, y_f)}. \quad (4)$$

We can see that by calculating the energy functions of factors in two cliques, only two variables θ_u and θ_b are required to be optimized.

C. Feature Function Designing

Following the above derivation, we now explicitly design the feature functions in the form of a unary term and a binary term. The unary term focuses on the reliability of individual tracklets, whereas the binary term considers the relationship between different pairs of tracklets.

1) *Unary Term*: Two kinds of information are taken into account when designing the feature functions for the unary term: the classification score S_f and the changing rate of the aspect ratio ΔR_f :

$$\Phi_u(x_f, y_f) = \mathbf{1}_{\{y_f=0\}}(|0 - S_f| + \mathbf{1}_{\{S_f > 0.95\}}\alpha_1) + \mathbf{1}_{\{y_f=1\}}(|1 - S_f| + \alpha_2 |1 - \Delta R_f|), \quad (5)$$

where

$$\mathbf{1}_{\{A=B\}} = \begin{cases} 1 & , \text{ if } A = B \\ 0 & , \text{ if } A \neq B \end{cases}. \quad (6)$$

Here, α_1 and α_2 are hyperparameters that are initialized heuristically and are adjusted by using a validation dataset. S_f comes directly from the output of the Faster R-CNN. $\mathbf{1}_{\{S_f > 0.95\}}$ lays extra punishment for the inactivation with classification scores higher than 0.95. To define ΔR_f specifically, we replace it by ΔR_i^t , where i denotes the index of the only node in the factor. Then, we have

$$\Delta R_i^t = \frac{w_i^t/h_i^t}{w_i^{t-1}/h_i^{t-1}}. \quad (7)$$

2) *Binary Term*: In our method, the binary term formulates the punishment for joint values of the two nodes contained in each factor. In [26], an assumption is given that the change of velocity should be basically the same between two tracking targets in a short time interval, i.e.

$$disp_i^t - disp_j^t = disp_i^{t-1} - disp_j^{t-1}, \quad (8)$$

where $disp_i^t$ is the center displacement of object i between frame t and frame $t-1$. This assumption have two implications:

- (i) The absolute velocity of pedestrians can be approximately regarded as a constant value during short time intervals. Hence, $disp_i^t - disp_i^{t-1}$ leads to the magnitude of camera motion.
- (ii) Sharp rotation and swing should not be involved in the camera motion.

We follow a similar assumption and make further improvement in the following four aspects:

- 1) The units of measure is unified when calculating the velocity by multiplying the frame rate ω of the sequence, i.e., $V_i^t = \omega(P_i^t - P_i^{t-1})$ where P denotes the center position of the object. Likely, we calculate the changing rate of velocity as $\Delta V_i^t = \omega(V_i^t - V_i^{t-1})$.
- 2) A coefficient $\tau = \frac{1}{h_i + h_j}$ is introduced to balance the weights, where h is the height of a tracked object. This design is proposed due to the observation that the position of a larger object tends to be estimated with worse performance.
- 3) The above assumption is extended to the changing rate of the object height $\Delta L_i^t = \omega \frac{\Delta h_i^t - \Delta h_i^{t-1}}{\Delta h_i^{t-1}}$, where $\Delta h_i^t = \omega \frac{h_i^t - h_i^{t-1}}{h_i^{t-1}}$. Note that the width of object is cast aside when calculating ΔL , the reason for which is depicted in Fig. 3.
- 4) When part of a tracking target moves out of sight, ΔL becomes unreliable due to the restriction of the image boundary. Therefore, an additional variable κ is introduced to address this concern, which takes 0 if the object is partially beyond the image boundary and takes 1 otherwise.

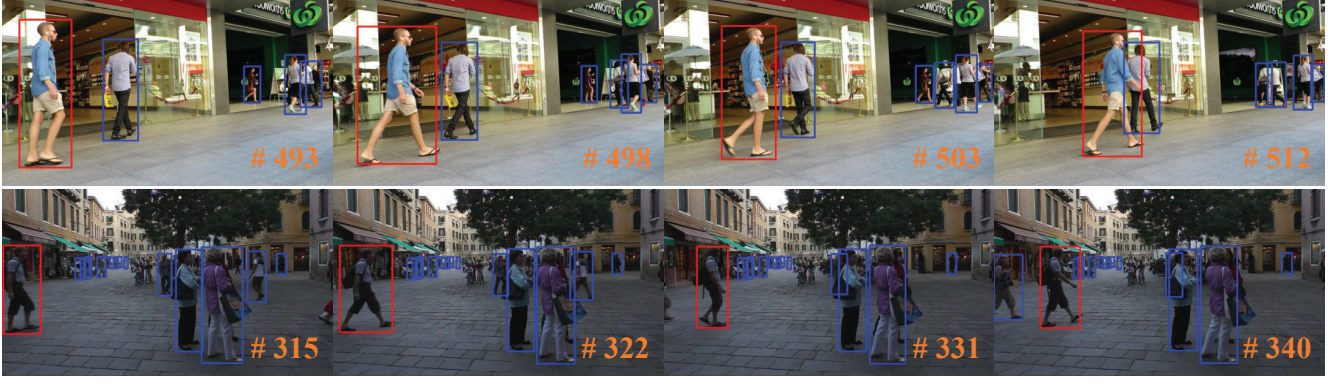


Fig. 3: Examples to explain for excluding the width term. The height of a pedestrian is stable regardless of the camera attitude, while the width of a pedestrian may change dramatically even in normal case because of the change in human postures.

Motivated by the above discussions, the feature functions of the binary term are designed as follows:

$$\Phi_b(x_f, y_f) = \mathbf{1}_{\{y_f=[1,1]\}} \left(\sum_{n \in \{x, y\}} \tau(\Delta V_{n,i} - \Delta V_{n,j})^2 + \beta \kappa | \Delta L_i - \Delta L_j | \right), \quad (9)$$

where β is a hyperparameter.

D. Inference and Training

To facilitate the inference and training of a CRF, we leverage two techniques to keep the number of CRF nodes fixed. The first technique, termed as hypothesis filtering, filters out extra objects with the highest classification scores when the detected objects outnumber a predefined value M . On the contrary, frames with nodes fewer than M are complemented by adding dummy nodes. The dummy nodes are artificially created to make the formulation hold, which are designed to exert no influence on the real nodes in a way that the formulae in Section III are regarded as multiplied by a boolean variable (which takes 1 when a factor contains no dummy nodes and takes 0 otherwise).

1) *CRF Inference*: The loopy belief propagation algorithm is adopted for dealing with the CRF inference task [4]. The main idea of the loopy belief propagation algorithm is demonstrated as follows, and we refer interested readers to [4], [28], [29] for further mathematical details.

The message flowing from a factor node to a variable node is defined as

$$M_{f,v}(x, y_v; \theta) = \sum_{y_f \in Y_f(y_v)} \left(e^{-E_f(x, y_f; \theta)} \prod_{\substack{v' \sim f \\ v' \neq v}} M_{v',f}(x, y_{v'}; \theta) \right), \quad (10)$$

where v and f denote a variable node and a factor node, respectively. $Y_f(y_u)$ is a subset of y_f 's domain that requires the node u to take the value y_u . $v \sim f$ signifies that an edge exists between v and f .

Conversely, the message flowing from a variable node to a factor node is defined as

$$M_{v,f}(x, y_v; \theta) = \frac{\prod_{\substack{f' \sim v \\ f' \neq f}} M_{f',v}(x, y_v; \theta)}{\sum_{y_v \in Y_v} \prod_{\substack{g \sim v \\ g' \neq f}} M_{f',v}(x, y_v; \theta)}. \quad (11)$$

The marginal distribution is then calculated by

$$p(y_v | x; \theta) = \frac{\prod_{f \sim v} M_{f,v}(x, y_v; \theta)}{\sum_{y_v \in Y_v} \prod_{f \sim u} M_{f,v}(x, y_v; \theta)}. \quad (12)$$

In order to get the optimal output y^* with respect to the maximum posterior probability (MAP), (10) and (11) are modified as

$$M_{f,v}(x, y_v; \theta) = \max_{y_f \in Y_f(y_v)} e^{-E_f(x, y_f; \theta)} \prod_{\substack{v' \sim f \\ v' \neq v}} M_{v',f}(x, y_{v'}; \theta), \quad (13)$$

$$M_{v,f}(x, y_v; \theta) = \frac{1}{2} \frac{\prod_{\substack{f' \sim v \\ f' \neq f}} M_{f',v}(x, y_v; \theta)}{\prod_{y_v \in Y_v} \prod_{\substack{g \sim v \\ g' \neq f}} M_{f',v}(x, y_v; \theta)}. \quad (14)$$

Finally, the output labels are obtained as follows:

$$y^* = [\max_{y_1} p(y_1 | x; \theta), \dots, \max_{y_M} p(y_M | x; \theta)]^T. \quad (15)$$

2) *CRF Training*: The purpose of CRF training is to get an estimation of the parameters using training samples $\{(x^1, y^1), \dots, (x^N, y^N)\}$. This problem can be naturally solved by Maximum Likelihood Estimation (MLE). Taking the first order derivative of the log likelihood of (4) and considering all N training samples, we have

$$\frac{\partial l(\theta)}{\partial \theta_{u/b}} = \sum_{n=1}^N \left(\sum_{f \in C_{u/b}} \Phi_{u/b}(x_f^n, y_f^n) - \sum_{f \in C_{u/b}} \sum_{y'_f} \Phi_{u/b}(x_f^n, y'_f) p(y'_f | x^n; \theta) \right) \quad (16)$$

where $p(y_f|x;\theta)$ is calculated in a similar way to (12):

$$p(y_f|x;\theta) = \frac{e^{-E_f(y_f)} \prod_{v \sim f} M_{v,f}(x, y_v; \theta)}{\sum_{y_f \in Y_f} [e^{-E_f(y_f)} \prod_{v \sim f} M_{v,f}(x, y_v; \theta)]}. \quad (17)$$

Applying the SGD algorithm with above gradients, the weights are updated with a fixed learning rate γ :

$$\theta' = \theta + [\gamma_u \frac{\partial l(\theta)}{\partial \theta_u}, \gamma_b \frac{\partial l(\theta)}{\partial \theta_b}]^T. \quad (18)$$

Algorithm 1: Workflow for tracking

Input: Images from frames to be tracked I^1, \dots, I^T ,
Public detection results D^1, \dots, D^T .

Output: Tracklets of objects tr_1, \dots, tr_K .

```

1 Initialize tracklets  $tr_1, \dots, tr_K$  by detections  $D^1$ ;
2 for  $t = 2, \dots, T$  do
3   Obtain regressing results  $x^t$  and classification
   scores  $S^t$  by using Tracktor++;
4   for tracklet index  $i = 1, \dots, K^t$  do
5     if  $S_i^t < 0.4$  then
6       Inactivate tracklet  $i$ ;
7     else
8       if tracklet length  $C_i \geq 2$  then
9         Calculate all the tracking information
         required in III-C;
10      end
11    end
12  end
13  if number of tracklets  $K^t > 10$  then
14    Cut down  $K^t$  to 10 by hypothesis filtering
    (III-D);
15  end
16  Calculate the unary and binary terms in the CRF
  (III-C);
17  Obtain the inactivation labels by using the loopy
  belief propagation algorithm (III-D1);
18  Inactivate tracklets by using the labels;
19  Do non-maximum suppression and reidentification.
20  Update  $tr_1, \dots, tr_k$ ;
21 end
22 return  $tr_1, \dots, tr_k$ .
```

IV. IMPLEMENTATION DETAILS

In this section, we first introduce the datasets used in practical tracking. The details for parameter estimation are then presented. Finally, the workflow and other details of practical tracking are introduced.

A. Datasets

Two popular datasets, MOT16 and MOT17 [30], are employed in this paper. Both these datasets provide official detection results that are called public detections. Researchers can also use private detections produced by their own detectors.

1) *MOT16*: The MOT16 dataset contains 14 video sequences of pedestrians with different resolutions, frame rates, lighting conditions, crowd density, and filming angles. They are evenly divided into a training dataset and a testing dataset. Each dataset has 4 sequences with moving cameras and 3 sequences with static cameras. The public detections are produced by using a DPM detector [31].

2) *MOT17*: The MOT17 dataset has the same video sequences as the MOT16. Notice that MOT17 provides three groups of public detections, which are produced by Faster R-CNN [2], DPM [31], and SDP [32] respectively, resulting in 42 sequences altogether. Trackers' performance on all 21 test sequences are averaged to get a generalized evaluation result. When tracking is performed with private detections, there is no difference in using the MOT16 dataset or the MOT17 dataset.

TABLE I: Parameters in CRF

Parameter	θ_u	θ_b	α_1	α_2	β
Value	0.98	0.12	1.05	1.20	10.80

TABLE II: Comparison of running speed (Hz)

Hypothesis number	3	6	10	15	Overall
Ours	6.80	5.51	2.82	1.67	2.22
Tracktor++	7.09	6.35	3.20	1.98	2.58

B. Parameter Estimation

It should be mentioned that there is no suitable existing dataset for training our model. In this case, a specific dataset is created on our own to facilitate the training of our CRF module. The training datasets of MOT16 and MOT17 are divided into two parts: one part with 40% video frames is used to generate the training dataset, and the other one serves as the validation dataset. The original Tracktor++ is applied to the first part and pick out the tracking errors produced by improper inactivation for tracklets. Frames with such errors are treated as negative samples. Note that 3 times more positive samples are randomly selected. The weights of the unary and binary terms are then trained by using the SGD algorithm with a learning rate of 1×10^{-2} for 30 epochs.

Experimental results have shown that directly using the trained weights gave rise to unpromising performance on the validation dataset. This phenomenon stems from two sources:

- (i) Tracktor++ itself is a powerful tracker so that the generated training dataset has limited capacity.
- (ii) The samples from the dataset do not strictly satisfy the premise of independent and identical distribution (i.i.d.).

Thus, we use the weights learned in the training phase as a starting point wherefrom heuristic adjustment is made. Here we first apply the initial values to the hyperparameters and manually select some obvious failing cases from the tracking results on the training dataset. We observe the value of each item in (5) and (6). Then α_1 is adjusted to balance the values between normal classification scores and high (> 0.95) classification scores. α_2 is adjusted to balance the values

TABLE III: MOT16 results (public detections)

	MOTA↑	IDF1↑	MOTP↑	MT↑	ML↓	FP↓	FN↓	IDS↓	Frag↓
Ours	57.0	58.3	79.1	158	267	2610	75337	538	1212
Tracktor++v2 [1]	56.2	54.9	79.2	157	272	2394	76844	617	1068
KCF16 [20]	48.8	47.2	75.7	120	289	5875	86567	906	1116
MOTDT [33]	47.6	50.9	74.8	115	291	9253	85431	792	1858
JCSTD [34]	47.4	41.1	74.4	109	276	8076	86638	1266	2697
AMIR [35]	47.2	46.3	75.8	106	316	2681	92856	370	598
YOONKJ [36]	47.0	50.1	75.8	125	317	7901	88179	627	945
DD_TAMA [37]	46.2	49.4	75.4	107	334	5126	92367	598	1127
DMAN [21]	46.1	54.8	73.8	132	324	7909	89874	532	1616
STAM [38]	46.0	50.0	74.9	111	331	6895	91117	473	1422
RAR16pub [39]	45.9	48.8	74.8	100	318	6871	91173	648	1992

TABLE IV: MOT17 results (public detections)

	MOTA↑	IDF1↑	MOTP↑	MT↑	ML↓	FP↓	FN↓	IDS↓	Frag↓
Ours	56.3	57.5	78.9	490	839	8672	236296	1668	3820
Tracktor++v2 [1]	56.3	55.1	78.8	498	831	8866	235449	1987	3763
LSST [40]	52.7	57.9	76.2	421	801	15884	246939	3711	8757
FAMNet [41]	52.0	48.7	76.5	450	787	14138	253616	3072	5318
YOONKJ [36]	51.4	54.0	77.0	500	878	29051	243202	2118	3072
STRN [42]	50.9	56.0	75.6	446	797	25295	249365	2397	9363
MOTDT [33]	50.9	52.7	76.6	413	841	24069	250768	2474	5317
DEEP_TAMA [37]	50.3	53.5	76.7	453	883	25479	252996	2192	3978
EDMT [43]	50.0	51.3	77.3	509	855	32279	247297	2264	3260
GMPHDOGM [44]	49.9	47.1	77.0	464	895	24024	255277	3125	3540
MTDF [45]	49.6	45.2	75.5	444	779	37124	241768	5567	9260

between classifications scores and the changing of aspect ratios. β is adjusted to balance the values between the changing rate of velocity and object height. Eventually, θ_u and θ_v are adjusted so that neither the unary term nor the binary term should be too much larger than each other. In fact, α_1 , α_2 and β can also be trained by using the SGD algorithm instead of being treated as hyperparameters. The final values for all the parameters in our method are listed in Table II.

C. Practical Tracking

The overall workflow for practical tracking with public detections is shown in Algorithm 1. Before performing the hypothesis filtering, all the tracklets with classification scores lower than 0.4 are inactivated. As for the predefined value M in III-D, we need to seek a decent balance between the handling capability of the CRF and the tracking speed. Notice that it is scarcely possible for a tracker to simultaneously inactivate more than 5 objects in a single frame. In this case, we double the number and set $M = 10$, meaning that 10 tracking hypotheses with the lowest classification scores are modelled as CRF nodes. Frames with objects less than 10 will be processed with dummy nodes as mentioned. For tracklets whose lengths are shorter than 3, we follow the convention in Tracktor++, i.e., a threshold (0.5) of classification score is selected to determine the inactivation.

To present a fair comparison with the baseline tracker, we wrote the experimental code based on the newly released code¹ provided by the authors of Tracktor++. Because of a retrained CNN network, the performance of the released code surpasses

that of the original paper. When comparing the experimental tracking performance in the following section, we refer to this version of tracker as Tracktor++v2, which is an alias used by its authors on the MOT16 and MOT17 results.

The computational complexity of the CRF module is $\mathcal{O}(n^2)$ in view of the number of CRF nodes. We test our tracker and the released code of Tracktor++ on a personal computer with an Intel i7-9700 CPU and a Nvidia GTX 2080ti GPU. The average running speed of both trackers with respect to sequence frames containing different number of tracking hypotheses is reported in Table I.

V. EXPERIMENTS

In this section, we first introduce the metrics used to evaluate the MOT performance. Then, quantitative results on MOT16 and MOT17 benchmarks are presented. After that, the tracking results are shown qualitatively to provide an intuitive understanding of our method. Finally, an extensive experiment is conducted to exhibit the extensibility of our method.

A. Evaluation Metrics

Evaluating the performance of an MOT tracker reasonably is a non-trivial task. Three evaluation systems, the CLEAR MOT metrics [3], the ID metrics [46] and some other classical metrics are used to verify the validity of our method. These metrics are regrouped into two categories as follows:

(i) Singular metrics.

- Multiple Object Tracking Precision (MOTP). MOTP describes the precision of bounding box regression, which mainly relies on the performance of the object detector.

¹https://github.com/phil-bermann/tracking_wo_bnw

TABLE V: MOT17 results (private detections)

	MOTA↑	IDF1↑	MOTP↑	MT↑	ML↓	FP↓	FN↓	IDS↓	Frag↓
Ours	58.9	60.4	78.1	609	669	20565	208680	2544	6459
Tracktor++v2	58.9	56.9	78.1	603	666	20640	208572	2853	6471

- Mostly Tracked (MT). The number of trajectories that are successfully tracked for more than 80% of its ground truth boxes.
- Mostly Lost (ML). The number of trajectories that fail to be tracked for more than 20% of its ground truth boxes.
- False Positives (FP).
- False Negatives (FN).
- Identification Switches (IDS).
- Fragments (Frag). The number of fragments in all trajectories.

(ii) Compound metrics.

- Multiple Object Tracking Accuracy (MOTA). Considering the number of False Positives (FP), False Negatives (FN), and ID Switches (IDS), MOTA is defined as

$$\text{MOTA} = 1 - \frac{\text{FP} + \text{FN} + \text{IDS}}{\text{GT}}, \quad (19)$$

where GT denotes the number of ground truth boxes.

- Identification F_1 (IDF1). IDF1 stands for the F_1 score of ID Precision (IDP) and ID Recall (IDR):

$$\text{IDF1} = 1 - \frac{2}{\frac{1}{\text{IDP}} + \frac{1}{\text{IDR}}} = \frac{2\text{IDTP}}{2\text{IDTP} + \text{IDFP} + \text{IDFN}}, \quad (20)$$

where IDTP, IDFP, and IDFN stands for ID True Positives, ID False Positives, and ID False Negatives respectively. Detailed definitions can be found in [46].

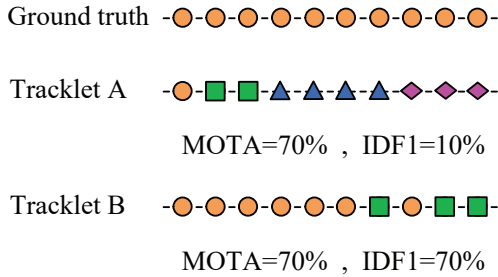


Fig. 4: The deficiency to use MOTA alone. Tracklet A and tracklet B have the same MOTA score, yet the latter one is intuitively better. This is because the CLEAR MOT metrics pay more attention to the coverage rate of the ground truth boxes, while ID metrics are able to depict more details about the ID information.

The compound metrics are chosen as the main indicators to evaluate trackers' performance. Although MOTA is a comprehensive metric, it is not enough to judge a trackers' performance only depending on MOTA. We illustrate the reason why MOTA should be combined with IDF1 in Fig. 4. The assumption is that all the objects are perfectly recognized whereas the identifications are improperly judged. Different

assumed identifications are represented by different shapes and colors.

B. Quantitative Analysis

We compare the proposed tracking method with TOP-10 online MOT trackers² with public detections on the MOT16 and MOT17 benchmarks. The experimental results are listed in Table III and Table IV. The up-arrow denotes the higher the better and the down-arrow means the opposite. The highest scores are marked in bold.

Taking MOTA and IDF1 scores as the first and second important metrics, our method achieves the best performance on both MOT16 and MOT17 benchmarks. Compared with the baseline method Tracktor++ on MOT16, the MOTA and IDF1 scores are increased by 0.8% and 3.4%, respectively. On MOT17, we increase the IDF1 score by 2.4%. In Table IV, the IDF1 score of our method performs better than the others' in evaluating a tracker's ability to maintain the identification of tracklets. This result is coherent with our improved approach for tracklet inactivation, which mitigates the problem of hypothesis drifting.

We further compare our tracker with Tracktor++ using private detections on the MOT17 benchmark, i.e., objects are detected by employing the retrained Faster R-CNN of both our tracker and Tracktor++. Such comparison is not done on MOT16 since the sequences in MOT16 are identical to those in MOT17. As is shown in Table V, we increase the IDF1 score by 3.5%. It is worth mentioning that the ID Switches (IDS) of our approach is less than that of the Tracktor++ in all three experimental setups, which further confirms that our method is important in stabilizing the ID information.

For a deeper insight of the experimental results, we count the number of IDS in each one of MOT17 test sequences, as is shown in Fig. 5. We see that our method alleviates the problem of ID Switch in both sequences with a static camera (01, 03, 08) and sequences with camera motion (06, 07, 12). The only test result with no IDS reduction is MOT17-14, the scenes in which rotate a lot and have a sharp left and right swing. In such a case, our assumption in subsection III-C does not hold well as in other video sequences.

We also make a comparison between the baseline tracker and our improved tracker in view of a significant MOT metric, the IDF1 score, in Fig. 6. Compared with IDS, the IDF1 score can better reflect the continuity and uniqueness of ID assignment and thus is an investigation focus of our method. It can be observed that our tracker achieves a higher IDF1 score than the baseline tracker in most test sequences on both MOT16 and MOT17 benchmarks. Note that our tracker is not

²We only consider the results on the MOT official website with published works. The TOP-10 list is up to the date when this paper was written.

superior on all the video sequences because of the domain diversity of MOT benchmark. The video sequences in MOT are captured under various environmental settings, such as different illumination conditions, different camera angles, with or without camera motion, etc. This means that we have to make a compromise on the parameters to achieve a generally decent performance for multiple domains. However, in real applications (e.g. intelligent surveillance), we scarcely need a tracker to cope with data from as many domains as in the MOT challenge. In other words, our method has more potential to be exploited than it seems on the benchmark performance.

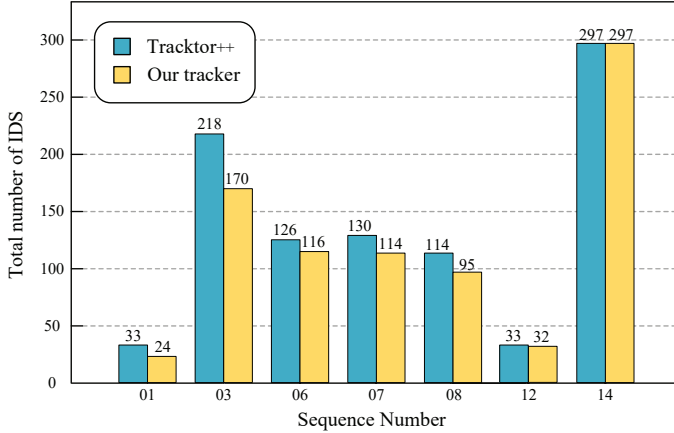
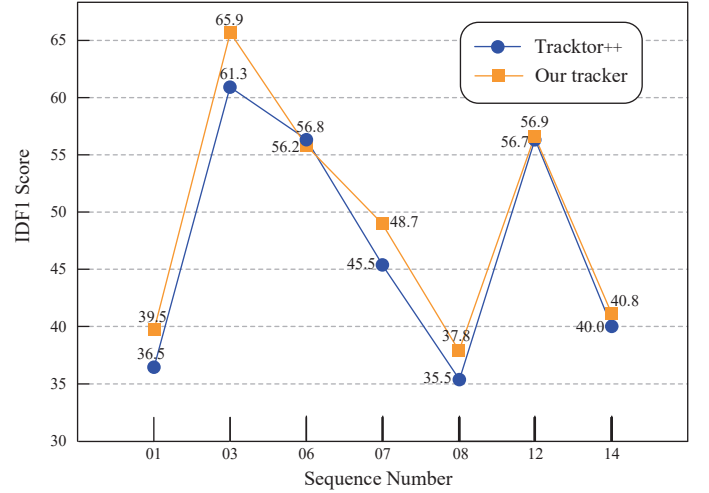


Fig. 5: Statistics of IDS in MOT17 test sequences (with private detections).

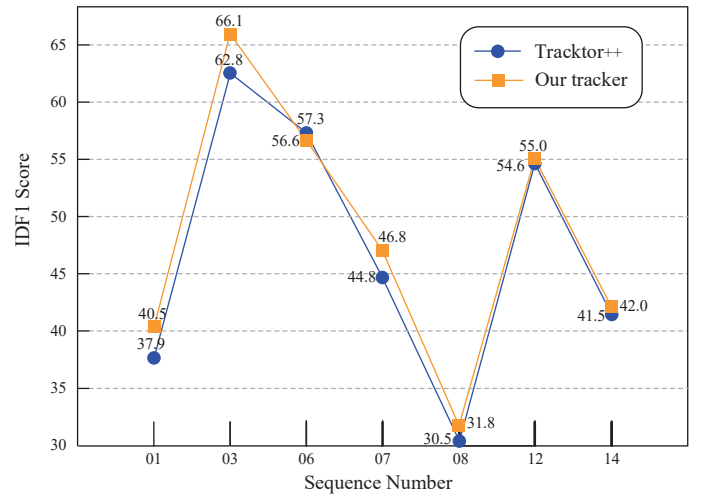
C. Qualitative Analysis

We visualize some of the representative tracking results (with public detections) in Fig. 7 to provide an intuitive understanding of our method. The tracking hypotheses to be noticed are marked with red arrows. For narrative convenience the hypotheses pointed by red arrows are dubbed as target people. In the 1st row, when the target person is leaving the image boundary at frame 358, its bounding box begins to drift to the man in black shirt. The tracker mistakes the fake target person as the original one and continues to track him without changing the tracking ID in later frames. By contrast, our improved tracker correctly inactivates the target person at frame 358. The newly emerging person in black shirt is then treated as a new tracking object so that a new tracking ID is assigned to him. Likewise, the target person in the 3rd row drifts to the man in suit at frame 680 and the target person in the 5th row drifts to the nearby woman at frame 779. It can be seen from the 4th and the 6th rows that our method kills such drifting trend by inactivating the tracklets in due course.

When an occluded object gradually enters the visual field, it is supposed to be either identified as a new track by the detector or reidentified as a previous track by a CNN network. However, neither of these circumstances would be accessible when the object is compulsively assigned a wrong ID due to nearby hypothesis drifting. Even worse, the tracker is unable to be aware of such an ID error since new position is regressed merely using the position in the previous frame. Our CRF



(a) MOT16



(b) MOT17

Fig. 6: Comparison of IDF1 scores on MOT benchmarks.

model handles this problem by telling the tracker to inactivate the tracklet promptly before drifting happens, making possible new detection and reidentification that would be suppressed otherwise.

It may be argued about the necessity to consider the inter-object relationship as we do, because hypothesis drifting can be recognized by discovering the sudden change of the position or size of a hypothesis. This argument does not hold when there is camera motion in the video sequences. On the contrary, our algorithm still works out in the existence of camera motion.

D. Extensive Experiment

Due to the fact that the proposed method is decoupled from the main tracking pipeline of Tracktor++, we can adapt it to other trackers that share a similar architecture with our baseline. To give an example, we conduct an extensive experiment on another state-of-the-art method CenterTrack [47] to exhibit the extensibility of our method.



Fig. 7: Some visualized tracking results. We pick video clips from MOT17-05, MOT16-06, and MOT16-07, all of which are video sequences with camera motion. The 1st, 3rd, and 5th rows are the tracking results by Tracktor++, while the 2nd, 4th, and 6th rows are our results. By observing the target indicated by the red arrow, we see that drifting could happen when occlusion occurs. Using a discrete CRF, we resolve such problems by reasonable judgement about when to inactivate a tracklet.

CenterTrack takes both the current frame and the previous frame as input and simultaneously predicts the object locations and the inter-frame offsets. A greedy matching algorithm is utilized to associate the detections and tracklets. To apply our method, we consider the inter-object relationship and remove the associated pairs that are denied by the CRF module. Then we re-associate the remaining unassigned detections and tracklets by using the greedy matching algorithm.

The unary term of the feature function is adapted into:

$$\Phi_u(x_f, y_f) = \mathbf{1}_{\{y_f=0\}} \frac{1}{D} + \mathbf{1}_{\{y_f=1\}} \alpha |1 - \Delta R_f|, \quad (21)$$

where D is the calculated distance between the center of the tracked position and the biased center (i.e. taking into account the predicted offset) of the detection. The binary term of the feature function is kept unchanged.

As is done in [47], the training set of MOT17 is split into a training set and a validation set. We tune the parameters only on the training set and evaluate the performance of our improved method on the validation set. By experiment, it is found that our tracker does not make obvious improvement over the baseline in all video sequences. This is attributed to two reasons: i) Our method mainly takes effect when the baseline tracker makes ID mistakes. For some of the videos, CenterTrack makes very few such mistakes. ii) Since this extensive experiment is designed to exhibit the potential and extensibility of our tracker, we do not deep dive into it. Therefore, we list the experimental results of three video sequences (05, 10, 11) which are relatively representative in Table VI. Compared with the baseline, our method is able to achieve a higher IDF1 score and make fewer ID switches.

For an intuitive understanding, some of the visualized

results are shown in Fig. 8. With the consideration of inter-object relationship, the CRF module contributes to killing the wrong ID assignment by detecting the abnormal changes of the tracking hypotheses in a tracklet. This can be seen by observing the behavioral differences between our tracker and CenterTrack at frames 433 \rightarrow 435, frames 526 \rightarrow 528, and frames 391 \rightarrow 393 respectively in the three video clips of Fig. 8.

TABLE VI: MOT17 results of the extensive experiment (public detections)

Method	Seq. 05		Seq. 10		Seq. 11	
	IDF1 \uparrow	IDS \downarrow	IDF1 \uparrow	IDS \downarrow	IDF1 \uparrow	IDS \downarrow
Ours	61.4	49	56.8	76	59.6	27
CenterTrack	60.2	52	55.8	78	58.8	28

VI. CONCLUSION

In this paper, the improper tracklet inactivation problem in Tracktor++ has been studied by using a discrete conditional random field to model the tracklets. The problem of varying CRF nodes has been handled, and dedicated feature functions have been designed. Our proposed algorithm is meaningful in that it can be extracted as a separate module and conveniently applied to other trackers with a similar architecture to Tracktor++, namely trackers remoulded from detectors. Experiments conducted on MOT16 and MOT17 benchmarks with both public and private detections have corroborated the effectiveness of the proposed method. The extensibility of our method is further validated by an extensive experiment on CenterTrack.

REFERENCES

- [1] P. Bergmann, T. Meinhardt, and L. Leal-Taixe, "Tracking without bells and whistles," in *Proceedings of the IEEE International Conference on Computer Vision*, 2019, pp. 941–951.
- [2] S. Ren, K. He, R. Girshick, and J. Sun, "Faster r-cnn: Towards real-time object detection with region proposal networks," pp. 91–99, 2015.
- [3] K. Bernardin and R. Stiefelhagen, "Evaluating multiple object tracking performance: the clear mot metrics," *EURASIP Journal on Image and Video Processing*, vol. 2008, pp. 1–10, 2008.
- [4] J. Pearl, "Probabilistic reasoning in intelligent systems: networks of plausible inference," 2014.
- [5] G. Ciaparrone, F. L. Sánchez, S. Tabik, L. Troiano, R. Tagliaferri, and F. Herrera, "Deep learning in video multi-object tracking: A survey," *Neurocomputing*, vol. 381, pp. 61–88, 2020.
- [6] A. A. Mekonnen and F. Lerasle, "Comparative evaluations of selected tracking-by-detection approaches," *IEEE Transactions on Circuits and Systems for Video Technology*, vol. 29, no. 4, pp. 996–1010, 2018.
- [7] A. Bewley, Z. Ge, L. Ott, F. Ramos, and B. Upcroft, "Simple online and realtime tracking," in *2016 IEEE International Conference on Image Processing (ICIP)*. IEEE, 2016, pp. 3464–3468.
- [8] H. W. Kuhn, "The hungarian method for the assignment problem," *Naval research logistics quarterly*, vol. 2, no. 1-2, pp. 83–97, 1955.
- [9] R. E. Kalman, "A new approach to linear filtering and prediction problems," *Journal of Fluids Engineering, Transactions of the ASME*, 1960.
- [10] N. Wojke, A. Bewley, and D. Paulus, "Simple online and realtime tracking with a deep association metric," in *2017 IEEE international conference on image processing (ICIP)*. IEEE, 2017, pp. 3645–3649.
- [11] Q. Zhou, B. Zhong, Y. Zhang, J. Li, and Y. Fu, "Deep alignment network based multi-person tracking with occlusion and motion reasoning," *IEEE Transactions on Multimedia*, vol. 21, no. 5, pp. 1183–1194, 2018.
- [12] P. Dai, X. Wang, W. Zhang, and J. Chen, "Instance segmentation enabled hybrid data association and discriminative hashing for online multi-object tracking," *IEEE Transactions on Multimedia*, vol. 21, no. 7, pp. 1709–1723, 2018.
- [13] Q. Bao, W. Liu, Y. Cheng, B. Zhou, and T. Mei, "Pose-guided tracking-by-detection: Robust multi-person pose tracking," *IEEE Transactions on Multimedia*, 2020.
- [14] F. Yu, W. Li, Q. Li, Y. Liu, X. Shi, and J. Yan, "POI: Multiple object tracking with high performance detection and appearance feature," in *European Conference on Computer Vision*. Springer, 2016, pp. 36–42.
- [15] H. Karunasekera, H. Wang, and H. Zhang, "Multiple object tracking with attention to appearance, structure, motion and size," *IEEE Access*, vol. 7, pp. 104423–104434, 2019.
- [16] Z. Fu, F. Angelini, J. Chambers, and S. M. Naqvi, "Multi-level cooperative fusion of gm-phd filters for online multiple human tracking," *IEEE Transactions on Multimedia*, vol. 21, no. 9, pp. 2277–2291, 2019.
- [17] Y. Lu, C. Lu, and C.-K. Tang, "Online video object detection using association LSTM," in *2017 IEEE International Conference on Computer Vision (ICCV)*. IEEE, 2017, pp. 2363–2371.
- [18] H. Sheng, J. Chen, Y. Zhang, W. Ke, Z. Xiong, and J. Yu, "Iterative multiple hypothesis tracking with tracklet-level association," *IEEE Transactions on Circuits and Systems for Video Technology*, vol. 29, no. 12, pp. 3660–3672, 2018.
- [19] J. F. Henriques, R. Caseiro, P. Martins, and J. Batista, "High-speed tracking with kernelized correlation filters," *IEEE Transactions on Pattern Analysis and Machine Intelligence*, vol. 37, no. 3, pp. 583–596, 2014.
- [20] P. Chu, H. Fan, C. C. Tan, and H. Ling, "Online multi-object tracking with instance-aware tracker and dynamic model refreshment," in *2019 IEEE Winter Conference on Applications of Computer Vision (WACV)*. IEEE, 2019, pp. 161–170.
- [21] J. Zhu, H. Yang, N. Liu, M. Kim, W. Zhang, and M.-H. Yang, "Online multi-object tracking with dual matching attention networks," in *Proceedings of the European Conference on Computer Vision (ECCV)*, 2018, pp. 366–382.
- [22] M. Danelljan, G. Bhat, F. S. Khan, and M. Felsberg, "ECO: Efficient Convolution Operators for Tracking," in *The IEEE Conference on Computer Vision and Pattern Recognition (CVPR)*. IEEE, 2017, pp. 6931–6939.
- [23] B. Yang and R. Nevatia, "An online learned CRF model for multi-target tracking," in *The IEEE Conference on Computer Vision and Pattern Recognition (CVPR)*. IEEE, 2012, pp. 2034–2041.
- [24] A. Heili, A. López-Méndez, and J.-M. Odobez, "Exploiting long-term connectivity and visual motion in crf-based multi-person tracking," *IEEE Transactions on Image Processing*, vol. 23, no. 7, pp. 3040–3056, 2014.
- [25] J. Xiang, G. Xu, C. Ma, and J. Hou, "End-to-end learning deep crf models for multi-object tracking," *IEEE Transactions on Circuits and Systems for Video Technology*, 2020.
- [26] H. Zhou, W. Ouyang, J. Cheng, X. Wang, and H. Li, "Deep Continuous Conditional Random Fields With Asymmetric Inter-Object Constraints for Online Multi-Object Tracking," *IEEE Transactions on Circuits and Systems for Video Technology*, vol. 29, no. 4, pp. 1011–1022, 2019.
- [27] F. R. Kschischang, B. J. Frey, and H.-A. Loeliger, "Factor graphs and the sum-product algorithm," *IEEE Transactions on Information Theory*, vol. 47, no. 2, pp. 498–519, 2001.
- [28] S. Nowozin and C. H. Lampert, "Structured learning and prediction in computer vision," *Foundations and Trends® in Computer Graphics and Vision*, vol. 6, no. 3–4, pp. 185–365, 2011.
- [29] C. Sutton and A. McCallum, "An introduction to conditional random fields," *Foundations and Trends® in Machine Learning*, vol. 4, no. 4, pp. 267–373, 2012.
- [30] A. Milan, L. Leal-Taixé, I. Reid, S. Roth, and K. Schindler, "Mot16: A benchmark for multi-object tracking," *arXiv preprint arXiv:1603.00831*, 2016.
- [31] P. F. Felzenszwalb, R. B. Girshick, D. McAllester, and D. Ramanan, "Object detection with discriminatively trained part-based models," *IEEE transactions on pattern analysis and machine intelligence*, vol. 32, no. 9, pp. 1627–1645, 2009.
- [32] F. Yang, W. Choi, and Y. Lin, "Exploit all the layers: Fast and accurate cnn object detector with scale dependent pooling and cascaded rejection classifiers," in *Proceedings of the IEEE conference on computer vision and pattern recognition*, 2016, pp. 2129–2137.
- [33] L. Chen, H. Ai, Z. Zhuang, and C. Shang, "Real-time multiple people tracking with deeply learned candidate selection and person re-identification," in *2018 IEEE International Conference on Multimedia and Expo (ICME)*. IEEE, 2018, pp. 1–6.



Fig. 8: Some visualized tracking results of the extensive experiment. The first two video clips come from MOT17-05 the third one comes from MOT17-10. The 1st, 3rd, and 5th rows are the tracking results by CenterTrack, while the 2nd, 4th, and 6th rows are our results. The tracking targets to be noticed are indicated by red arrows.

- [34] W. Tian, M. Lauer, and L. Chen, "Online multi-object tracking using joint domain information in traffic scenarios," *IEEE Transactions on Intelligent Transportation Systems*, vol. 21, no. 1, pp. 374–384, 2020.
- [35] A. Sadeghian, A. Alahi, and S. Savarese, "Tracking the untrackable: learning to track multiple cues with long-term dependencies," in *The IEEE International Conference on Computer Vision (ICCV)*, Oct 2017.
- [36] K. Yoon, J. Gwak, Y.-M. Song, Y.-C. Yoon, and M.-G. Jeon, "OneShotDA: online multi-object tracker with one-shot-learning-based data association," *IEEE Access*, vol. 8, pp. 38 060–38 072, 2020.
- [37] Y.-C. Yoon, D. Y. Kim, K. Yoon, Y.-m. Song, and M. Jeon, "Online multiple pedestrian tracking using deep temporal appearance matching association," *arXiv preprint arXiv:1907.00831*, 2019.
- [38] Q. Chu, W. Ouyang, H. Li, X. Wang, B. Liu, and N. Yu, "Online multi-object tracking using cnn-based single object tracker with spatial-temporal attention mechanism," in *Proceedings of the IEEE International Conference on Computer Vision*, 2017, pp. 4836–4845.
- [39] K. Fang, Y. Xiang, X. Li, and S. Savarese, "Recurrent autoregressive networks for online multi-object tracking," in *2018 IEEE Winter Conference on Applications of Computer Vision (WACV)*. IEEE, 2018, pp. 466–475.
- [40] W. Feng, Z. Hu, W. Wu, J. Yan, and W. Ouyang, "Multi-object tracking with multiple cues and switcher-aware classification," *arXiv preprint arXiv:1901.06129*, 2019.
- [41] P. Chu and H. Ling, "Famnet: Joint learning of feature, affinity and multi-dimensional assignment for online multiple object tracking," in *Proceedings of the IEEE International Conference on Computer Vision*, 2019, pp. 6172–6181.
- [42] J. Xu, Y. Cao, Z. Zhang, and H. Hu, "Spatial-temporal relation networks for multi-object tracking," in *Proceedings of the IEEE International Conference on Computer Vision*, 2019, pp. 3988–3998.
- [43] J. Chen, H. Sheng, Y. Zhang, and Z. Xiong, "Enhancing detection model for multiple hypothesis tracking," in *Proceedings of the IEEE Conference on Computer Vision and Pattern Recognition Workshops*, 2017, pp. 18–27.
- [44] Y.-M. Song, K. Yoon, Y.-C. Yoon, K. C. Yow, and M. Jeon, "Online multi-object tracking with GMPHD filter and occlusion group management," *IEEE Access*, vol. 7, pp. 165 103–165 121, 2019.
- [45] Z. Fu, F. Angelini, J. Chambers, and S. M. Naqvi, "Multi-level cooperative fusion of gm-phd filters for online multiple human tracking," *IEEE Transactions on Multimedia*, vol. 21, no. 9, pp. 2277–2291, 2019.

- [46] E. Ristani, F. Solera, R. Zou, R. Cucchiara, and C. Tomasi, “Performance measures and a data set for multi-target, multi-camera tracking,” in *European Conference on Computer Vision workshop on Benchmarking Multi-Target Tracking*. Springer, 2016, pp. 17–35.
- [47] X. Zhou, V. Koltun, and P. Krähenbühl, “Tracking objects as points,” *arXiv preprint arXiv:2004.01177*, 2020.